arXiv:1207.1022v1 [cond-mat.soft] 4 Jul 2012

The Effect of Particle Strength on the Ballistic Resistance of Shear Thickening Fluids

Oren E. Petel,[1, a)] Simon Ouellet,[2] Jason Loiseau,[1] Bradley J. Marr,[1] David L. Frost,[1] and Andrew J. Higgins[1]

[1)] *McGill University, Department of Mechanical Engineering, Montréal, Québec, Canada*

[2)] *Defence Research and Development Canada Valcartier, Val-Bélair, Québec, Canada*

(Dated: 5 July 2012)

The response of shear thickening fluids (STFs) under ballistic impact has received considerable attention due to its field-responsive nature. While efforts have primarily focused on the response of traditional ballistic fabrics impregnated with fluids, the response of pure STFs to penetration has received limited attention. In the present study, the ballistic response of pure STFs is investigated and the effect of fluid density and particle strength on ballistic performance is isolated. The loss of ballistic resistance of STFs at higher impact velocities is governed by particle strength, indicating the range of velocities over which they may provide effective armor solutions.

Keywords: Shear Thickening Fluid, Ballistic Impact, Penetration, Particulate Suspension, Material Strength Effects

---

[a)] oren.petel@mail.mcgill.ca

There is considerable interest in producing novel flexible armour systems by embedding shear thickening fluids (STFs) in ballistic fabrics[1–4]. These fluids are field responsive and can undergo a sudden fluid-solid transition under certain stimulii[5–8]. Extensive dynamic characterizations of STFs have been conducted at low stresses, primarily with rheometers[5,6] or split-Hopkinson pressure bars[9], which are not directly relevant to the dynamic high stress environment of a ballistic impact event. Recent experimental and analytical investigations of dense particulate suspensions under high-speed plate loading, effectively a one-dimensional ballistic impact, demonstrated that bulk dynamic strength effects resulted from a mesoscopic deformation leading to the formation of force-carrying chains within the suspended particles[10–13]. In the present study, we investigate the dominant role of the particle strength in determining the ballistic response of STFs through variations of the suspended particle materials.

While the ballistic response of hybrid fluid-fabric armor concepts has previously been tested in various configurations[2–4], the fluid-fabric coupling complicates identifying the ballistic response of the STFs themselves. For instance, ballistic studies have demonstrated that embedding fabrics with STFs increased the protection provided by those fabrics under ballistic testing[2–4]; however, a loss of performance is seen among impregnated fabrics when multiple layers and higher penetration velocities are considered, where the neat Kevlar fabrics outperform the embedded fabrics on an absolute basis[3]. Attributing this loss of performance to either the fluid or fabric component is difficult due to the coupling between the components of the system. As such, a thorough investigation of the ballistic response of pure STFs is necessary to elucidate their strength limitations at these extreme strain rates and stresses.

Kalman et al.[4] demonstrated that increased ballistic performance of impregnated Kevlars correlated to the material strength of the embedded particles, whereby introducing silica particles resulted in a higher ballistic limit than introducing softer polymethalmethacrylate particles into the fabrics. Demonstrating the primary importance of particle strength effects in the STF response, it was found that impregnating Kevlar fabrics with particles which were either suspended in a fluid (as a STF) or introduced with a solvent and dried were comparably effective at increasing the ballistic limit of the fabrics investigated.

During a ballistic impact event, the penetration process involves a complex stress state surrounding the projectile, with significant compressive and shear stresses. Under these con-

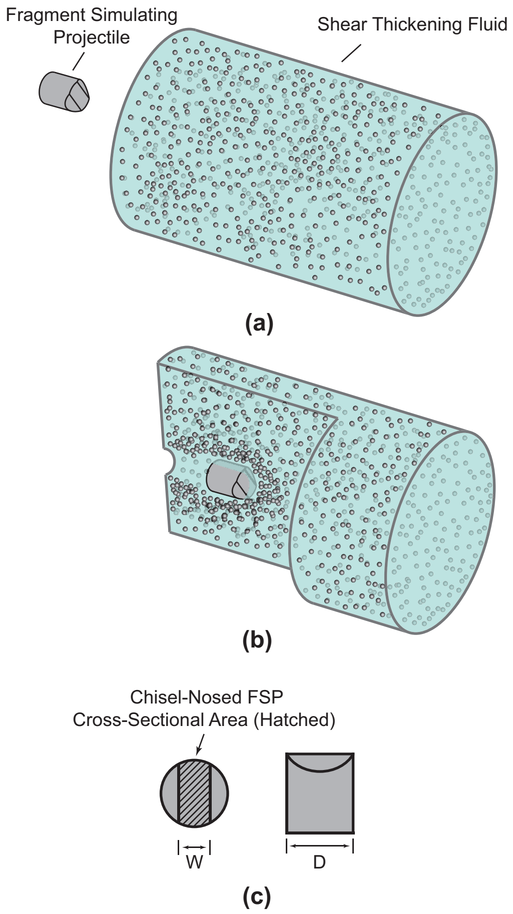
Fragment Simulating Projectile
Shear Thickening Fluid
(a)
(b)
Chisel-Nosed FSP Cross-Sectional Area (Hatched)
W
D
(c)

FIG. 1. Schematic of an STF suspension (a) in equilibrium prior to ballistic penetration and (b) a sectioned view of the projectile penetrating the suspension and the related mesostructural changes to the particle distribution. (c) Top and side views of a chisel-nosed FSP. The hatched region on the top view schematic represents the chisel-nosed cross-sectional area of the FSP.

ditions, in additional to the traditional shear thickening mechanism[8], a compression-induced clustering of particulates[10,11], analogous to granular jamming[14], may result in extensive particle force chains forming around the projectile (Fig. 1). Prior ballistic studies considered traditional STFs where the strength of the solid particulate (silica or polymers) was exceeded by the pressures generated in the ballistic impacts investigated[1–4]. The *in situ* formation of force chains implies that the ballistic limitations of STFs should be directly related to the strength of the suspended particles. If particle fracture occurs during force chain formation, high arresting stresses cannot be maintained on the projectile leading to a drop in the ballistic resistance of the suspension.

We investigate this hypothesis by studying the ballistic penetration of several STFs, a

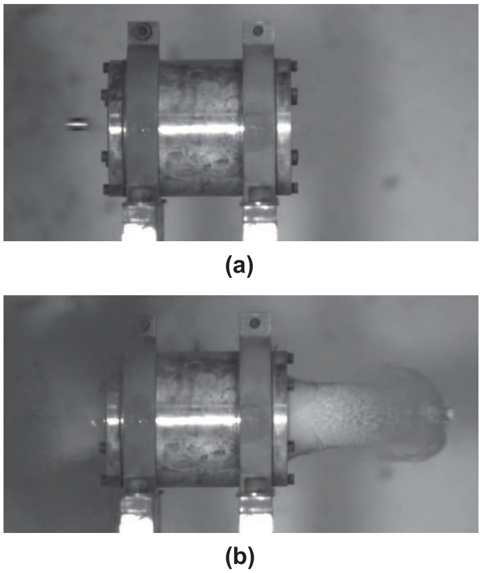

FIG. 2. Photographs of the FSP (a) entering and (b) exiting the test capsule.

dilute suspension, and neat ethylene glycol (the suspending medium for all of the mixtures under consideration). The suspended particulate phase of the STFs was varied in a manner that interrogates the influence of the material strength of the particles on penetration resistance. The experimental ballistic penetration results are presented in reference to a simple density-based penetration model to highlight the strength limitations of the various STFs.

The penetration resistance was investigated through the ability of the fluids to decelerate a 17 grain (1.1 g) chisel-nosed mild steel NATO-standard fragment simulating projectile (FSP), shown schematically in Fig. 1. The samples were tested in a cylindrical aluminum capsule with an internal diameter of 38 mm and a length of 64 mm. Mylar diaphragms (0.1 mm thick), which were found to have a negligible influence on the experimental results, were used to confine the fluid samples in the capsules during the experiments. The target capsule was positioned close to the end of the smooth-bore gas-gun barrel in order to minimize the projectile yaw at the impact face. The incident and exit velocities of the FSP were measured with a Photron SA5 ultra high-speed camera operating at 20,000 fps. A set of images taken of the incident and exiting projectile are shown in Fig. 2. The deceleration of the FSP through the various mixtures was investigated over an incident velocity range of 310 to 830 m/s.

The investigation involved several mixtures, the proportions of which are given in Table I. The components of the various mixtures included liquid ethylene glycol, silica (Fiber Optic

TABLE I. Summary of the mixture compositions investigated in the present study.

Sample Name	**Liquid Component**	**Solid Component(s)**	**Solid Mass Fraction (%)**	**Solid Volume Fraction (%)**	**Density (g/cm^3)**	**STF**
EG	Ethylene Glycol	n/a	n/a	n/a	1.11	No
54 CS	Ethylene Glycol	Cornstarch	62.0	54.0	1.35	Yes
21 SiC	Ethylene Glycol	Silicon Carbide	44.2	21.5	1.57	No
61 SiO_2	Ethylene Glycol	Silicon Dioxide	72.5	61.5	1.57	Yes
61 Mix	Ethylene Glycol	Silicon Dioxide Silicon Carbide	50.2 25.5	47.6 13.9	1.76	Yes

Center, monodisperse spheres, $d = 1$ μm), α-silicon carbide (Washington Mills, irregular morphology, $d_{mean} = 5$ μm), and cornstarch (Fleichmann, $d_{mean} = 10$ μm). The three types of solid components in the STFs have drastically different material strengths. In order of increasing yield strength, the materials are cornstarch, silica and silicon carbide. It should be noted that the silica particles had a micro-porous structure (with 16% void by volume), resulting in a bulk particle density of 1.85 g/cm^3. The bulk particle density of the silica particles considered in the present study is consistent with the density of the silica used in previous ballistic experiments involving silica-based STFs[2]. This significant void fraction in the silica particles would have an adverse affect the yield strength of the silica particles.

Of the mixtures that are summarized in Table I, three of the mixtures investigated exhibit discontinuous shear thickening behaviors: 54 CS, 61 SiO_2, and 61 Mix. The 21 SiC mixture, a dilute suspension that did not exhibit STF behavior, was used for a density-matched comparison to the 61 SiO_2 mixture that did behave as a STF. The measured velocity decrements of the FSP are compared between test mixtures as a means of evaluating the competition between the mixture density and the material strength of the suspended solid phase as the dominant factor in the ballistic resistance of the various STFs.

A simple analytical hydrodynamic penetration model, assuming ideal plug formation and no material strength in the target, can be used to investigate density-dominated penetration behavior. The assumptions inherent in this model are: (*i*) the projectile drives a plug through the target with a cross-sectional area equal to that of the chisel nose (Fig. 1c), (*ii*) the target material has no material strength, and (*iii*) the impact and penetration process is perfectly plastic, resulting in identical final velocities of the projectile and plug. The assumption concerning the cross-sectional area of the plug accounts for the divergence of material around the projectile tip. The model can therefore be adequately described by conserving momentum through the equation,

$$\rho_p L_p \cdot V_i = (\rho_p L_p + \rho_t L_t A_r) \cdot V_f \tag{1}$$

where L is the length, ρ is the density, A_r is the area ratio of the chisel nose to the projected area of the FSP, V_i is the incident projectile velocity, V_f is the projectile velocity on exit, and the subscripts p and t refer to the projectile and target respectively. The area ratio can be determined from geometric considerations such that,

$$A_r = 1 - \tfrac{1}{\pi} \cdot (\theta - sin\theta) \tag{2}$$

$$\theta = 2cos^{-1}\left(\tfrac{W}{D}\right) \tag{3}$$

where D is the diameter of the FSP and W is the width of the chisel nose, 5.38 mm and 2.54 mm, respectively, for a 17 grain chisel-nosed FSP.

While this penetration model is extremely simple, it predicts that for a given target density and capsule size, the velocity decrement through the sample normalized by the incident projectile velocity is independent of the incident velocity (Fig. 3), which accurately reproduces the experimental trends observed. The invariance of this normalized velocity decrement provides a means of investigating the effect of dynamic material strength on ballistic penetration by comparing the experimental results with a purely density-based penetration behavior.

The result of the simple model, calculated for a target with the density of ethylene glycol (EG), is represented in Fig. 3 by a solid line. Experimentally, three fluids tested in the present study (EG, 21 SiC, and 54 CS) were found to follow the trend predicted by the simple model, despite the fact that 54 CS is an STF. The two mixtures which deviated from this behavior were the 61 SiO_2 and 61 Mix, both STFs (see Table I).

The 61 SiO_2 and 61 Mix mixtures showed similar deviations from a purely density dominated behaviour as predicted by the model. At lower velocities, both mixtures were effective at stopping or decelerating the projectile. At higher velocities, their normalized deceleration asymptoted toward a density dominated deceleration, independant of further increases in the incident projectile velocity. Therefore, the results point to a transition in behavior, where the low velocity penetration is dominated by the dynamic material strength and higher velocity penetration is dominated by the mixture density.

This transition is particularly evident when a comparison is made between two mixtures with the same density, 61 SiO_2 and 21 SiC, the former being a STF. The convergence in projectile deceleration at high impact velocities is evident when the variation in deceleration of each mixture is plotted without normalization (Fig. 4). At low impact velocities, the ballistic results suggest that the onset of a dynamic material strength in 61 SiO_2 dominates and enhances its resistance to penetration. However, at higher impact velocities, this effect is less important and the bulk mixture density dominates the dynamic response, evidenced by the convergence of the ballistic results for the mixtures.

Comparing the results for the three STFs on the basis of their transition to a target density-dominated behavior in Fig. 3, the effect of the particle strength is clearly evident. While the mixtures containing ceramic particles (61 SiO_2 and 61 Mix) have a noticeable material strength response at lower impact velocities, no such effect is seen in the results with the 54 CS STF. Due to the low yield strength of cornstarch, the 54 CS mixture exhibits a density-dominated response similar to the trend from the hydrodynamic penetration model and the 21 SiC and EG experiments.

Considering the results of the 61 SiO_2 and 61 Mix (Fig. 3), the particle strength effect on ballistic penetration is most pronounced. Both of these mixtures have identical solid phase volume fractions, the only difference being the proportion of silica and silicon carbide in the two mixtures (Table I). The addition of a small volume of silicon carbide extended the incident velocity range over which the material strength dominated the ballistic response

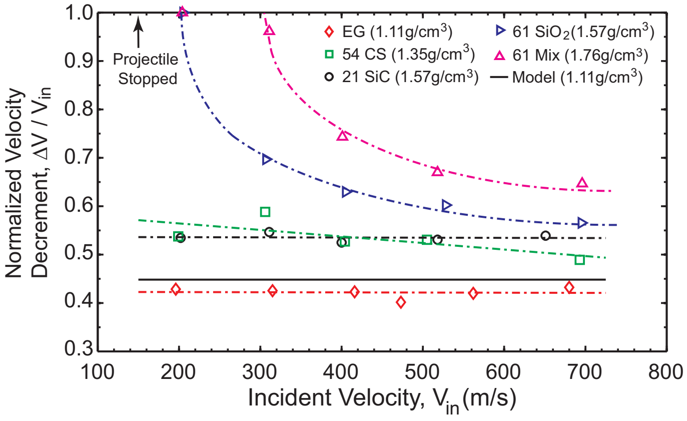

FIG. 3. A comparison of the change in FSP velocity normalized by the incident velocity of the FSP for the various mixtures tested.

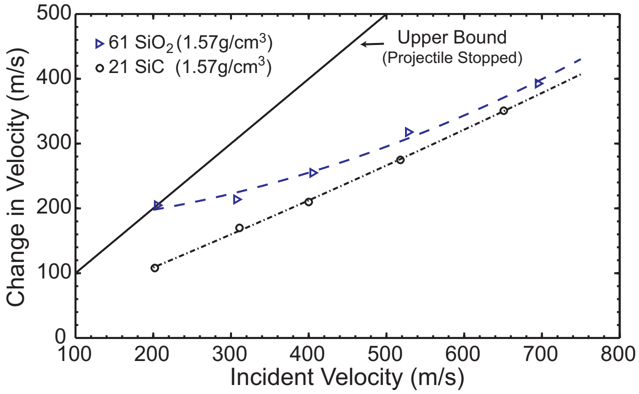

FIG. 4. A comparison of the penetration response of two mixtures with the same bulk density, 21 SiC and 61 SiO_2, that isolates the shear thickening contribution to the ballistic resistance offered by the fluids.

of the STF. The higher yield strength of the silicon carbide particles in comparison to that of porous silica led to the increased ballistic resistance of the 61 Mix STF. This increased resistance resulted in delaying the transition from material strength to density-dominated penetration resistance to higher incident projectile velocities.

A fluid-solid transition can be triggered in dense suspensions when the rate of relative particle displacement exceeds the rate of particle relaxation, leading to the development of stress-bearing disordered structures, which has been shown to occur under both shear[5–7] and high-speed uniaxial compression[10–13]. Consequently, increasing the loading rate beyond the critical rate for the onset of this transition could not explain the diminished effect of shear thickening on penetration resistance at higher impact velocities as suggested by Tan et al[3]. If we consider that the dynamic response involves mesostructural reorganization and the formation of clustered particles, the strength of the suspended particles becomes an important parameter in the dynamic response of the STF. If the dynamic strength of the particles is exceeded, local particle fracture and deformation would result in a loss of strength in the stiffened mixture. Under the extreme stresses associated with ballistic impact events, localized particle fracturing can be important. Once the strength of the materials forming the clusters within the STF is exceeded, the material response is dominated simply by its bulk density.

The authors would like to thank Jacques Blais of DRDC Valcartier for his assistance in conducting the experiments. This work was conducted with the support of Hamid Bennadi of Stedfast Ltd., the Natural Sciences and Engineering Research Council of Canada, and the Department of National Defence under project DNDPJ 385687-09.

REFERENCES

[1] L. E. Gates Jr., Air Force Materials Laboratory, AFML-TR-68-362 (1968).

[2] Y. S. Lee, E. D. Wetzel, and N. J. Wagner, Journal of Materials Science **38**, 2825 (2003).

[3] V. B. C. Tan, T. E. Tay, and W. K. Teo, International Journal of Solids and Structures **42**, 1561 (2005).

[4] D. P. Kalman, R. L. Merrill, N. J. Wagner, and E. D. Wetzel, Applied Materials & Interfaces **1**, 2602 (2009).

[5] R. L. Hoffman, Transactions of the Society of Rheology **16**, 155 (1972).

[6] H. A. Barnes, Journal of Rheology **33**, 329 (1989).

[7] A. A. Catherall, J. R. Melrose, and R. C. Ball, Journal of Rheology **44**, 1 (2000).

[8] N. J. Wagner and J. F. Brady, Physics Today **62**, 27 (2009).

[9] A. S. Lim, S. L. Lopatnikov, N. J. Wagner, and J. W. Gillespie Jr., Rheologica Acta **49**, 879 (2010).

[10] O. E. Petel and A. J. Higgins, Journal of Applied Physics **108**, 114918 (2010).

[11] O. E. Petel, D. L. Frost, A. J. Higgins, and S. Ouellet, Physical Review E **85**, 021401 (2012).

[12] O. E. Petel, D. L. Frost, A. J. Higgins, and S. Ouellet, AIP Conference Proceedings **1426**, 1459 (2012).

[13] O. E. Petel, D. L. Frost, A. J. Higgins, and S. Ouellet, AIP Conference Proceedings **1426**, 1495 (2012).

[14] A. J. Liu and S. R. Nagel, Annual Review of Condensed Matter Physics **1**, 347 (2010).